Single π production in neutrino nucleus scattering

E. Hernández,[1] J. Nieves,[2] and M. J. Vicente Vacas[3]

[1]*Departamento de Física Fundamental e IUFFyM,*
Universidad de Salamanca, E-37008 Salamanca, Spain.
[2]*Instituto de Física Corpuscular (IFIC), Centro Mixto CSIC-Universidad de Valencia,*
Institutos de Investigación de Paterna, Apartado 22085, E-46071 Valencia, Spain
[3]*Departamento de Física Teórica e IFIC, Centro Mixto Universidad de Valencia-CSIC,*
Institutos de Investigación de Paterna, Apartado 22085, E-46071 Valencia, Spain

We study 1π production in both charged and neutral current neutrino nucleus scattering for neutrino energies below 2 GeV. We use a theoretical model for one pion production at the nucleon level that we correct for medium effects. The results are incorporated into a cascade program that apart from production also includes the pion final state interaction inside the nucleus. Besides, in some specific channels coherent π production is also possible and we evaluate its contribution as well. Our results for total and differential cross sections are compared with recent data from the MiniBooNE Collaboration. The model provides an overall acceptable description of data, better for NC than for CC channels, although theory is systematically below data. Differential cross sections, folded with the full neutrino flux, show that most of the missing pions lie in the forward direction and at high energies.

PACS numbers: 13.15.+g,25.30.Pt

arXiv:1304.1320v2 [hep-ph] 24 May 2013

I. INTRODUCTION

A correct understanding of neutrino-nucleus interactions is crucial to minimize systematic uncertainties in neutrino oscillation experiments [1]. Most of the new generation of neutrino experiments are exploring neutrino-nuclear scattering processes at intermediate energies. Recently the MiniBooNE Collaboration has published one pion production cross sections on mineral oil by $\nu_\mu/\bar{\nu}_\mu$ neutrinos with energies below $2\,\text{GeV}$. The data include neutral-current (NC) single π^0 production by ν_μ and $\bar{\nu}_\mu$ [2], as well as ν_μ induced charged-current (CC) charged pion production [3] and neutral pion production [4]. These are the first pion production cross sections to be measured since the old bubble chamber experiments carried out at Argonne National Laboratory (ANL) [5, 6] and Brookhaven National Laboratory (BNL) [7]. The latter were measured on deuterium where nuclear effects are small [8, 9]. The main contribution to MiniBooNE data comes from ^{12}C and this poses an extra problem to theoretical calculations as a direct test of any fundamental production model is difficult since in-medium modifications of the production mechanisms and final state interaction (FSI) effects on the produced pions are important.

These new data show interesting deviations from the predictions of present theoretical models [10]. In Ref. [11], the NuWro Monte Carlo event generator is used to study $NC\ \pi^0$ production data in nuclei. A simple theoretical model is used to describe the pion production on the nucleon. No background terms are considered, and the coherent pion production is calculated using the Rein-Sehgal model [12], which is not appropriate at low energies [13–15]. A fair agreement for neutrino induced reactions and a little worse agreement for the antineutrino case are obtained. CC single pion production off ^{12}C for neutrino energies up to $1\,\text{GeV}$ has been analyzed in Ref. [16]. The pion production theoretical model is here more complete [17] but nuclear effects have been included only in a very simplified manner. Only total cross sections were calculated and approximately agree with MiniBooNE data for the π^+ channel and deviate more for the π^0 channel. The most comprehensive approach till now, with both a quite complete microscopic description of the pion production on the nucleon[1] and the nuclear medium effects, can be found in Ref. [20]. There, the Giessen Boltzmann-Uehling-Uhlenbeck (GiBUU) model is used finding that total cross sections measured by MiniBooNE are higher than theoretical ones for neutrino energies above $0.8 \sim 0.9\,\text{GeV}$ and obtaining also some discrepancies in the differential cross sections. The study of [20] is limited only to the incoherent part of the CC induced reaction, and no comparison with the MiniBooNE NC data of Ref. [3] is performed. However, such comparison was presented/discussed in NUFACT and NUINT conferences in 2009 [21, 22].

In this paper, we address the problem of $\nu(\bar{\nu})$-induced pion production, both for CC and NC driven processes, using a more sophisticated theoretical model, although it is restricted to relatively low pion energies. We start from the one-pion production model on nucleons from Refs. [9] and [17] which includes the Δ resonance mechanisms, but also the background terms generated by the leading order chiral Lagrangian. In order to extend the model to higher energies above the Δ resonance region for which it was originally developed, we add a new resonant contribution corresponding to the $D_{13}(1520)$. According to Ref. [18], this resonance, besides the $\Delta(1232)$, is the only one playing a significant role for neutrino energy below $2\,\text{GeV}$. Next, we have also incorporated several nuclear medium corrections that directly affect the production mechanisms. Apart from Pauli-blocking and Fermi motion we take into account the important corrections that stem from Δ resonance properties modification inside the nuclear medium. Finally, the pion FSI is also relevant for the comparison with the experiment, as a number of pions will be absorbed or rescattered, possibly changing their charge, in their way out of the nucleus. For the inclusion of these effects, we shall follow Ref. [23] where a simulation code for inclusive pion nucleus reactions was developed. In some specific channels coherent π production in ^{12}C is also possible and to evaluate its contribution, we use the model of Ref. [13] but with the newer nucleon-to-Δ form factors extracted in Ref [9], where a simultaneous fit to ANL and BNL data, accounting for deuteron effects as well, was carried out.

The paper in organized as follows: In Sec. II we introduce our model for π production induced by $\nu(\bar{\nu})$ at the nucleon level, the relevant modifications for in-medium calculations and briefly describe the implementation of the π FSI. A comparison with MiniBooNE data is shown in Sec. III and the main conclusions of this work are collected in Sec. IV. In Appendix A, the details on the D_{13} contribution to pion production by neutrinos at the nucleon level is included.

---

[1] The model [18] includes the weak excitation of several resonance contributions and their subsequent decay into πN. The vector couplings are taken directly over from the MAID analysis [19], while the axial couplings are obtained from partial conservation of the axial current (PCAC). For the necessary background terms, the vector part is again determined using the MAID analysis as a basis. For the axial part (including the vector-axial interference) it was then assumed that it is proportional to the vector part. The proportionality constant is adjusted to the old bubble chamber ANL and BNL data, neglecting small deuteron effects.

II.   MODEL FOR ONE PION PRODUCTION INDUCED BY NEUTRINOS

A.   Pion production at the nucleon level

The starting point is the model of Ref. [17] for one pion production on the nucleon which is depicted diagrammatically in Fig. 1. It contains the dominant Δ resonance term and background terms required by chiral symmetry. In total
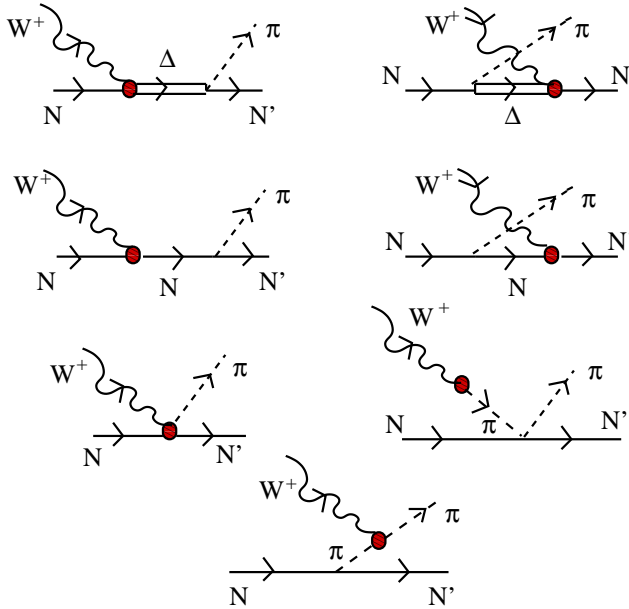

FIG. 1.   Model for the $W^+ N \to N' \pi$ reaction. We have direct and crossed $\Delta(1232)-$ and nucleon pole terms, contact and pion pole contribution, and the pion-in-flight term. We denote these contributions by: ΔP, $C\Delta P$, NP, CNP, CT, PP and PF, respectively.

we have direct and crossed $\Delta(1232)-$ (first row) and nucleon$-$ (second row) pole terms, contact and pion pole contribution (third row) and finally the pion-in-flight term. The background terms are the leading contributions of a $SU(2)$ nonlinear σ model. Those were supplemented with well known form factors in a way that respected both conservation of the vector current (CVC) and PCAC hypotheses. Their contribution is sizeable even at the $\Delta(1232)$resonance peak and it turns out to be dominant near pion threshold.

For the nucleon to Δ weak transition matrix element the form factor parametrization of Refs. [24, 25] was taken[2] in [17]. A total of four vector and four axial form factors are needed. The three vector form factors $C_3^V(q^2)$, $C_4^V(q^2)$, $C_5^V(q^2)$ were determined from photo and electroproduction data whereas $C_6^V(q^2) = 0$ from CVC. The vector form factors from Ref. [26] were used. For the axial part, Adler's model [27] in which $C_3^A(q^2) = 0$, $C_4^A(q^2) = -C_5^A(q^2)/4$, and PCAC, that requires $C_6^A(q^2) = -C_5^A(q^2)M^2/(m_\pi^2 - q^2)$ with M, m_π the nucleon and pion masses, were used. Thus, there is only one axial form factor to be determined, namely the dominant $C_5^A(q^2)$. For the latter, the parametrization of Ref. [28] was assumed in [17] and the unknown parameters $C_5^A(0)$ and $M_{A\Delta}$ were fitted to the flux averaged, $W < 1.4\,\mathrm{GeV}$, $\nu_\mu p \to \mu^- p \pi^+$ q^2 differential cross section measured at ANL [6]. Here, W stands for the final pion-nucleon invariant mass.

While the results for different total and differential cross sections were in good agreement with ANL data [5, 6], the total cross sections were smaller than the experimental data measured at BNL [7]. BNL and ANL data seemed to be incompatible. It was pointed out in Ref. [29] that this problem might originate from two factors: First, both ANL and BNL data were measured on deuterium. Deuteron structure effects in the $\nu_\mu d \to \mu^- \Delta^{++} n$ reaction were estimated in Ref [8] to produce a reduction in the cross section from $5 - 10\%$ and most analysis, including Ref. [17], neglected that effect. Second, both experiments suffered from neutrino flux uncertainties that in Ref. [29] were estimated to be 20% for ANL and 10% for BNL. Following the work of Ref. [29], a combined fit of $C_5^A(q^2)$ to both ANL and BNL $p\pi^+$ data, including in both cases full deuteron effects and the flux normalization uncertainties, was carried out in [9]. In this latter fit, a simpler pure dipole parametrization $C_5^A(q^2) = C_5^A(0)/(1 - q^2/M_{A\Delta}^2)^2$ was used obtaining

---

[2] Note that the C_5^A sign is quoted incorrectly in Ref. [24] (see comment in Ref. [24, 25]).
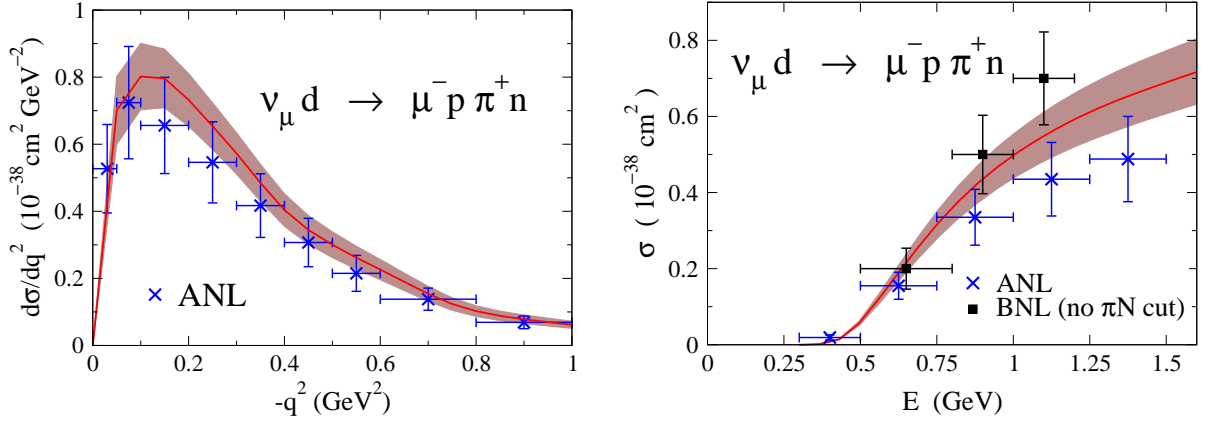
FIG. 2. Comparison of the theoretical model [9] results (solid line) to ANL [6] and BNL [7] experimental data. Theoretical 68% confidence level bands are also shown. Data include a systematic error (20% for ANL and 10% for BNL data) that has been added in quadratures to the statistical published errors. The theoretical results and ANL data include a $W < 1.4\,\mathrm{GeV}$ cut in the final πN invariant mass.
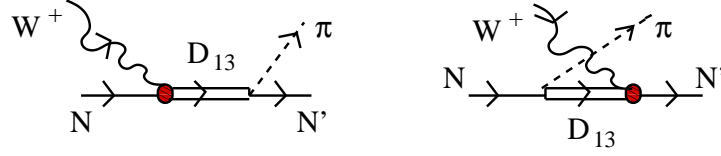

FIG. 3. $D_{13}(1520)$ contributions to $W^+ N \to N'\pi$. We have direct (DP) and crossed (CDP) $D_{13}(1520)-$pole contributions.

$C_5^A(0) = 1.00 \pm 0.11$ and $M_{A\Delta} = 0.93 \pm 0.07\,\mathrm{GeV}$. The results from that fit, compared to ANL and BNL data, are shown in Fig. 2. The above mentioned parameterization for $C_5^A(q^2)$ is the one we are using in the present calculation.

For the present calculation, and in order to better compare with MiniBooNE data, we need to extend the model up to 2 GeV neutrino energies, where higher mass resonances could play a role. According to Ref. [18], and apart from the Δ, only the $D_{13}(1520)$ resonance gives a significant contribution in that region. We shall include in our model the two new contributions depicted in Fig. 3. All the details of the calculation of these diagrams are given in Appendix A. We would like to remark that as the D_{13} has isospin $1/2$, it does not contribute in the $p\pi^+$ channel and thus, it does not affect the previous fit.

The differential neutrino-nucleon cross section with respect to the pion energy E_π and the angle between the pion momentum and the neutrino beam θ_π is given for a CC process by [17]

$$\frac{d\sigma(\nu N \to l^- N'\pi)}{d\cos\theta_\pi dE_\pi} = 2\pi \frac{G_F^2}{4\pi^2} \frac{|\vec{k}_\pi|}{|\vec{k}|} \frac{1}{4M} \frac{1}{(2\pi)^3} \int d\Omega' dE' |\vec{k}'| \frac{1}{2E_{N'}} \delta(E_N + q^0 - E_\pi - E_{N'}) \mathcal{L}_{\mu\sigma}(k, k') \mathcal{W}^{\mu\sigma}(p_N, q, k_\pi).$$

(1)

G_F is the Fermi decay constant. k, k' and k_π are the neutrino, final charged lepton and final pion four-momenta respectively. Besides, $q = k - k'$ is the four-momentum transferred, and $E_N = \sqrt{M^2 + \vec{p}_N^2}$, $E_{N'} = \sqrt{M^2 + (\vec{p}_N + \vec{q} - \vec{k}_\pi)^2}$ are the initial and final nucleon energies. The lepton and hadronic tensors are given by

$$\mathcal{L}_{\mu\sigma}(k, k') = k_\mu k'_\sigma + k_\sigma k'_\mu - k \cdot k' g_{\mu\sigma} + i\epsilon_{\mu\sigma\alpha\beta} k'^\alpha k^\beta$$

(2)

$$\mathcal{W}^{\mu\sigma}(p_N, q, k_\pi) = \overline{\sum_{\text{spins}}} \left\langle N'\pi | j_{cc+}^\mu(0) | N \right\rangle \left\langle N'\pi | j_{cc+}^\sigma(0) | N \right\rangle^*$$

(3)

with $\epsilon_{0123} = +1$ and the metric $g_{\mu\nu} = (+, -, -, -)$, and where in the hadronic tensor a sum over final spins and an average over initial ones is done. The $j_{cc+}^\mu(0)$ current contains all contributions in Fig. 1, see Refs. [9, 17] for details, plus the new D_{13} contributions of Fig. 3 that are given in Appendix A. A similar expression is obtained for an NC process in which we have a neutrino in the final state (see [17]).

B. In-medium production

For incoherent production on a nucleus we have to sum the contribution to the cross section of all nucleons in the nucleus[3]. Assuming the nucleus can be described by its density profile $\rho(r) = \rho_p(r) + \rho_n(r)$, and using the local density approximation, the initial differential cross section at the nucleus level for a pion production channel $N'\pi$, prior to any pion FSI, is then

$$\frac{d\sigma}{d\cos\theta_\pi dE_\pi} = \int d^3r \sum_{N=n,p} 2 \int \frac{d^3p_N}{(2\pi)^3} \, \theta(E_F^N(r) - E_N) \, \theta(E_N + q^0 - E_\pi - E_F^{N'}(r)) \frac{d\sigma(\nu N \to l^- N'\pi)}{d\cos\theta_\pi dE_\pi}, \qquad (4)$$

where $E_F^N(r) = \sqrt{M^2 + (k_F^N(r))^2}$, being $k_F^N(r) = (3\pi^2\rho_N(r))^{1/3}$ the local Fermi momentum for nucleons of type N. To compare with experiment, we have to convolute the above expression with the neutrino flux $\Phi(|\vec{k}|)$

$$\frac{d\sigma}{d\cos\theta_\pi dE_\pi} = \int d|\vec{k}| \, \Phi(|\vec{k}|) \, 4\pi \int r^2 \, dr \sum_{N=n,p} 2 \int \frac{d^3p_N}{(2\pi)^3} \, \theta(E_F^N(r) - E_N) \, \theta(E_N + q^0 - E_\pi - E_F^{N'}(r)) \frac{d\sigma(\nu N \to l^- N'\pi)}{d\cos\theta_\pi dE_\pi}. \qquad (5)$$

From there, we obtain

$$\frac{d\sigma}{d|\vec{k}|4\pi r^2 \, dr \, d\cos\theta_\pi \, dE_\pi} = \Phi(|\vec{k}|) \sum_{N=n,p} 2 \int \frac{d^3p_N}{(2\pi)^3} \, \theta(E_F^N(r) - E_N) \, \theta(E_N + q^0 - E_\pi - E_F^{N'}(r)) \frac{d\sigma(\nu N \to l^- N'\pi)}{d\cos\theta_\pi dE_\pi}. \qquad (6)$$

Apart from modifications discussed in what follows, the above differential cross section is used in our simulation code to generate, in a given point inside the nucleus and by neutrinos of a given energy, pions with a certain charge, energy and momentum direction.

Defining $P = q - k_\pi$ (the four momentum transferred to the nucleus) and writing $d^3p_N = d\cos\vartheta_N \, d\phi_N \, |\vec{p}_N| E_N dE_N$, where the angles are referred to a system in which the Z axis is along $\vec{P}$, we can integrate in the ϑ_N variable using the energy delta function present in $\frac{d\sigma(\nu N \to l^- N'\pi)}{d\cos\theta_\pi dE_\pi}$. The final result is

$$\frac{d\sigma}{d|\vec{k}|4\pi r^2 \, dr \, d\cos\theta_\pi \, dE_\pi} = \Phi(|\vec{k}|) \int d\Omega' dE' |\vec{k}'| \Bigg\{ \sum_{N=n,p} \frac{G_F^2}{512\pi^7} \frac{|\vec{k}_\pi|}{|\vec{P}| \, |\vec{k}|} \theta(E_F^N(r) - \mathcal{E}) \, \theta(-P^2) \, \theta(P^0) \, \mathcal{L}_{\mu\sigma}(k, k')$$

$$\int_0^{2\pi} d\phi_N \int_{\mathcal{E}}^{E_F^N(r)} dE_N \mathcal{W}^{\mu\sigma}(p_N, q, k_\pi)\Bigg|_{\cos\vartheta_N = \cos\vartheta_N^0} \Bigg\}, \qquad (7)$$

where

$$\cos\vartheta_N^0 = \frac{P^2 + 2E_N P^0}{2|\vec{p}_N||\vec{P}|}, \quad \mathcal{E}' = \frac{-P^0 + |\vec{P}|\sqrt{1 - 4M^2/P^2}}{2}, \quad \mathcal{E} = \max\{M, E_F^{N'} - P^0, \mathcal{E}'\}. \qquad (8)$$

To speed up the computational time, we approximate the last two integrals in Eq.(7) by

$$\int_0^{2\pi} d\phi_N \int_{\mathcal{E}}^{E_F^N(r)} dE_N \mathcal{W}^{\mu\sigma}(p_N, q, k_\pi)\Bigg|_{\cos\vartheta_N = \cos\vartheta_N^0} \approx 2\pi(E_F^N(r) - \mathcal{E})\mathcal{W}^{\mu\sigma}(\tilde{p}_N, q, k_\pi)\Bigg|_{\cos\vartheta_N = \cos\vartheta_N^0} \qquad (9)$$

where $\tilde{p}_N$ is evaluated at the value $\tilde{E}_N = (E_F^N(r) + \mathcal{E})/2$, (middle of the integration interval), with the corresponding $\cos\tilde{\vartheta}_N^0$ (that deduced from Eq. (8) using $E_N = \tilde{E}_N$ and $|\vec{p}_N| = \sqrt{\tilde{E}_N^2 - M^2}$), and $\tilde{\phi}_N$ is set to zero. Similar approximations were done, and shown to be sufficiently accurate, in Refs. [30–33] to study total inclusive and total inclusive pion production in photon and electron nuclear reactions. In the study in Ref. [34] of total inclusive neutrino induced cross section this kind of simplification was also used. We have checked that the approximation of Eq. (9)

---

[3] For coherent production one should sum amplitudes [13].

induces uncertainties at most of 5%, independently of $\tilde{\phi}_N$. Other choices to fix $\tilde{\phi}_N$ produce small variations of the order of 1-2%. With this approximation, we find

$$\frac{d\sigma}{d|\vec{k}|4\pi r^2 \, dr \, d\cos\theta_\pi \, dE_\pi} \approx \Phi(|\vec{k}|) \int d\Omega' dE' |\vec{k}'| \left\{ \sum_{N=n,p} \frac{G_F^2}{256\pi^6} \frac{|\vec{k}_\pi|}{|\vec{P}| \, |\vec{k}|} \left(E_F^N(r) - \mathcal{E}\right) \theta\left(E_F^N(r) - \mathcal{E}\right) \theta(-P^2)\,\theta(P^0) \right.$$
$$\left. \times \mathcal{L}_{\mu\sigma}(k,k') \mathcal{W}^{\mu\sigma}(\tilde{p}_N, q, k_\pi) \right\}. \tag{10}$$

Eq.(10) includes explicitly Fermi motion of the initial nucleon and Pauli blocking of the final nucleon but there are other important in-medium corrections, that we discuss in the following, that have to be included. The above expression is equivalent to Eqs. (2) and (25) of Ref. [34], where among others, the 1p1h1π excitations contribution to the total inclusive neutrino-nucleus cross sections was evaluated.

C.   In medium corrections to pion production and final state interaction

Given the dominant role played by the ΔP contribution and since Δ properties are strongly modified in the nuclear medium [13, 32, 35–41] a more proper treatment of the Δ contribution is needed. Here, we follow Ref. [32] and modify the Δ propagator in the ΔP term as

$$\frac{1}{p_\Delta^2 - M_\Delta^2 + iM_\Delta\Gamma_\Delta} \rightarrow \frac{1}{\sqrt{s} + M_\Delta} \frac{1}{\sqrt{s} - M_\Delta + i(\Gamma_\Delta^{\text{Pauli}}/2 - \text{Im}\Sigma_\Delta)},$$

with $s = p_\Delta^2$, $\Gamma_\Delta^{\text{Pauli}}$ the free Δ width corrected by Pauli blocking of the final nucleon, for which we take the expression in Eq.(15) of Ref. [42], and $\text{Im}\Sigma_\Delta$ the imaginary part of the Δ self-energy in the medium. For the mass we shall keep its free value. While there are some corrections to the mass coming both from the real part of the self-energy and RPA sums, together they induce changes smaller than the precision in the present experiments and the uncertainties due to our limited knowledge of the nucleon to Δ transition form factor $C_5^A(q^2)$, see discussion in Sec. II.E of Ref. [34].

The evaluation of Σ_Δ is done in Ref. [36] where the imaginary part is parametrized as

$$-\text{Im}\Sigma_\Delta = C_Q \left(\frac{\rho}{\rho_0}\right)^\alpha + C_{A_2} \left(\frac{\rho}{\rho_0}\right)^\beta + C_{A_3} \left(\frac{\rho}{\rho_0}\right)^\gamma,$$

with $\rho_0 = 0.17\,\text{fm}^{-3}$. The C_Q, α, C_{A_2}, β and C_{A_3}, γ coefficients can be found in Eq.(4.5) and Table 2 of Ref. [36]. They are parametrized as a function of the kinetic energy of a pion that would excite a Δ of the corresponding invariant mass and are valid in the range $85\,\text{MeV} < T_\pi < 315\,\text{MeV}$. Below $85\,\text{MeV}$ the contributions from C_Q and C_{A_3} are rather small and we take them from Ref. [42], where the model was extended to low energies. The term with C_{A_2} shows a very mild energy dependence and we still use the parameterization from Ref. [36] even at low energies. For T_π above 315 MeV, we have kept these self-energy terms constant and equal to their values at the bound. The uncertainties in these pieces are not very relevant there because the $\Delta \rightarrow N\pi$ decay becomes very large and dominant.

The terms in C_{A_2} and C_{A_3} are related to the two-body absorption $WNN \rightarrow NN$ and three-body absorption $WNNN \rightarrow NNN$ channels respectively. On the other hand the C_Q term gives rise to a new $WN \rightarrow N\pi$ contribution inside the nuclear medium and thus it has to be taken into account beyond its role in modifying the Δ propagator. This new contribution has to be added incoherently and we implement it in a approximate way by taking as amplitude square for this process the amplitude square of the ΔP contribution multiplied by

$$\frac{C_Q(\rho/\rho_0)^\alpha}{\Gamma_\Delta^{\text{Free}}/2}. \tag{11}$$

Our final model for production is then given in Eq.(10) with the modifications in the hadronic tensor just mentioned.

Once the pion is produced inside the nucleus, it starts propagating and it suffers interactions with the medium. To evaluate them we follow Ref. [23], where a computer simulation code was developed to describe inclusive pion nucleus reactions (quasielastic, single charge exchange, double charge exchange and absorption). We take into account P- and S-wave pion absorption, and P-wave quasielastic scattering on a single nucleon. The P- wave interaction is mediated by the Δ resonance excitation where the different contributions to the imaginary part of its self-energy give rise to pion two- and three-nucleon absorption and quasielastic processes. After a quasielastic interaction the pions change direction and may change charge. The intrinsic probabilities for each of the above mentioned reactions were evaluated microscopically as a function of the density and we use the local density approximation to evaluate them in finite

nuclei. In between collisions the pions are treated as classical particles and in the present calculation we shall assume they propagate in straight lines. All details of the simulation can be found in Ref. [23]. We should remark that this approach to π FSI has been extensively and successfully used in the study of many processes such as hypernuclear decays [43], π absorption [44], photon [31, 45] and electron [33] induced nuclear processes (like π production) or muon capture [46]. Furthermore, it has been extensively used in their analysis by the successive Kamiokande collaborations. See, e.g. Refs. [47–49].

D. Coherent production

In some of the channels there is a contribution from coherent π production. We evaluate it with the model of Ref. [13], using the $C_5^A(q^2)$ form factor obtained in Ref [9]. Cross sections for the T2K and MiniBooNE fluxes obtained with this new form factor were given in [41]. The model for coherent pion production is based on the microscopic model for pion production off the nucleon of Ref. [17] that as already mentioned, besides the dominant Δ pole contribution, takes into account the effect of background terms required by chiral symmetry. Our coherent production model does not incorporate the D_{13} contribution that we expect to produce only a small correction.

The main nuclear effects, namely, medium corrections on the Δ propagator and the final pion distortion, are included. As found in similar calculations [39, 50, 51], the modification of the Δ self-energy inside the nuclear medium strongly reduces the cross section, while the final pion distortion mainly shifts the peak position to lower pion energies.

We should stress that the model of Ref. [13] is more reliable than the Rein-Sehgal approach [12] for the energies of interest in this work. In particular, it greatly improves on the description of angular distributions of the outgoing pion with respect to the direction of the incoming neutrino [13, 15].

III.   RESULTS FOR PION PRODUCTION IN NEUTRINO NUCLEUS SCATTERING AND COMPARISON WITH MINIBOONE DATA

In this section we compare our predictions with data recently obtained by the MiniBooNE Collaboration for ν_μ induced CC [3, 4] and $\nu_\mu/\bar{\nu}_\mu$ induced NC [2] pion production in mineral oil (CH_2).

A. CC production

We start by showing results for the total unfolded cross sections for charged current one-pion production. In Fig. 4, we compare our results with the data by the MiniBooNE Collaboration for a final π^+. We take into account the contribution on ^{12}C and that on the two hydrogens. There is also a small coherent contribution on ^{12}C that we have evaluated as described above. Our total result agrees well with data at low neutrino energies, but is below data for neutrino energies above $0.9\,\text{GeV}$.

The D_{13} contribution is only noticeable above $E_\nu = 1.2\,\text{GeV}$. At around $E_\nu = 2\,\text{GeV}$, it makes some 8% of the total contribution. It will play a minor role for observables that are convoluted over the MiniBooNE neutrino flux as the latter peaks at around $0.6\,\text{GeV}$. On the other hand, in the whole energy range shown, the C_Q term (Eq. (11)) produces changes always smaller than 10%. In Fig. 5, we show the effect of varying $C_5^A(0)$ within the uncertainties in its determination, using BNL and ANL data, in Ref.[9]. We find effects at the 10% level. The highest value seems to be favored by the MiniBooNE data. We should remind here that if flux uncertainties were ignored, BNL and ANL data would not be compatible [29]. Taken at face value, the figure suggests that MiniBooNE data would support BNL results. This would also imply larger values of $C_5^A(0)$ closer to the PCAC prediction, as suggested in Ref. [20]. However, one should be cautious given the number of uncertainties in both experiment and theoretical models.

Similar results, consistently below data, are obtained for the case of CC π^0 production, see Fig. 6. As in the previous case, the role of the D_{13} resonance or the C_Q corrections are small.

In Fig. 7, we compare the differential $\frac{d\sigma}{dT_\pi}$ cross section for $CC\ 1\pi^+$ production by ν_μ, calculated with the MiniBooNE flux from Ref. [3]. In the left panel, we show the different contributions to the full model, including the coherent part. The model predicts less high energy pions than the experiment for T_π above $0.15\,\text{GeV}$. The combined effect of quasielastic scattering and pion absorption through Δ excitation depletes the $0.15 \sim 0.4\,\text{GeV}$ region. As a result the strength moves down to $0.8\,\text{GeV}$. The shape of the calculated cross section is dominated by the ^{12}C contribution and both the coherent part and the hydrogen contribution peak at higher energies but, they are too small to compensate for the missing high energy pions. On the right panel we also show the effect of not including the C_Q correction of
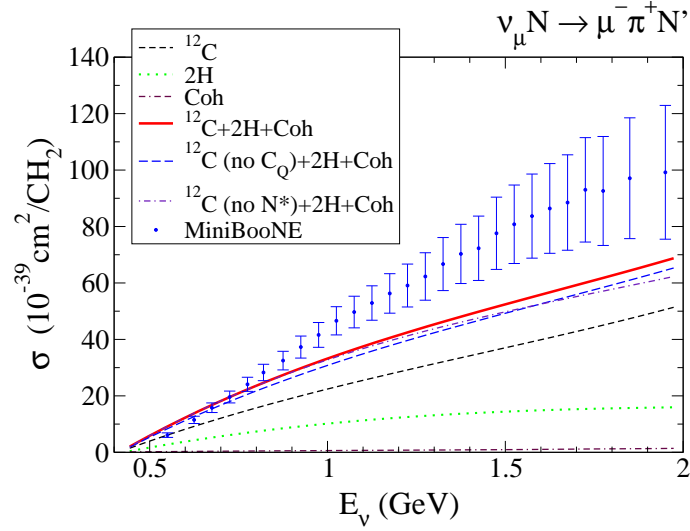
FIG. 4. $1\pi^+$ total production cross section for ν_μ CC interaction in mineral oil. Short-dashed line: ^{12}C contribution. Dotted line: H_2 contribution. Double-dashed dotted line: Coherent contribution (see main text). Solid line: Total contribution. Long-dashed line: Same as solid line but without the C_Q contribution of Eq. (11). Dashed-dotted line: Same as solid line but without the contribution from the D_{13} resonance contribution. Data taken from Ref. [3].
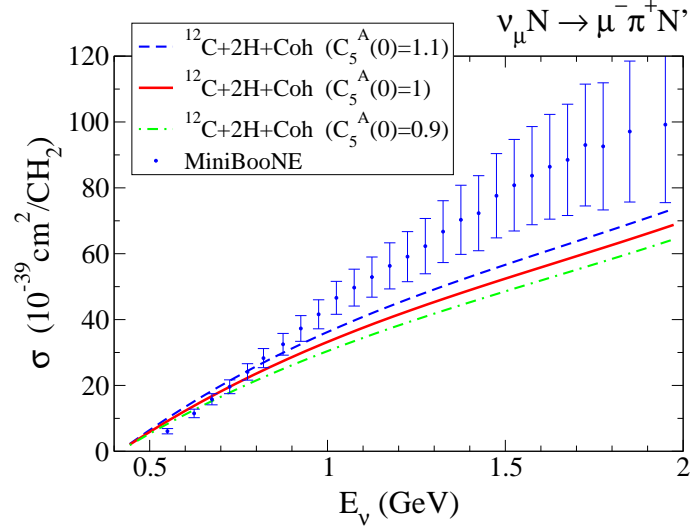

FIG. 5. $1\pi^+$ total production cross section for ν_μ CC interaction in mineral oil. Solid line: Our full model with $C_5^A(0) = 1$. Dashed line: Full model with $C_5^A(0) = 1.1$. Dashed-dotted line: Full model with $C_5^A(0) = 0.9$.

Eq. (11). We can see, that it little affects the cross section and/or the shape of the pion kinetic energy differential distribution.

From the above discussion we might expect a better agreement with data when FSI effects are neglected. Indeed, as can be seen on the right panel of Fig. 7, the experimental shape could be reproduced by artificially removing the FSI of the pion. Of course, this has little sense as FSI is really there. Removing FSI completely would lead to total cross section values that are too high at low neutrino energies, where the theoretical model is more reliable. FSI effects could be reduced by considering the so called "formation zone" [11], that among other effects includes the propagation of the Δ before decaying into a πN pair. Of course, the "formation zone" could be adjusted to reproduce data. These kind of modifications of the FSI could be difficult to justify, they might be in conflict with much other phenomenology and may somehow serve to hide our ignorance on the relevant dynamics. Even when they could help reproducing some observable, if we lack a correct understanding of the physical mechanisms responsible for them, they might lead to wrong predictions for other observables sensible to other kinematics, dynamical mechanisms or nuclear corrections.
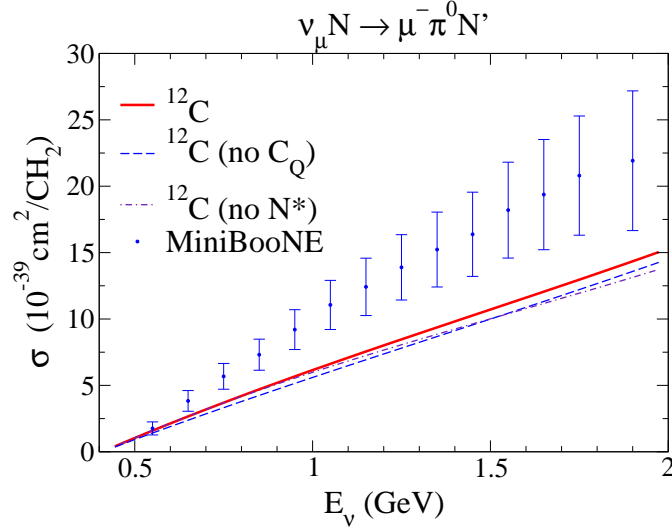
FIG. 6. $1\pi^0$ total production cross section for ν_μ CC interaction in mineral oil. In this case there is no contribution from the H_2 and there is no coherent contribution. Captions as in Fig. 4. Data from Ref. [4].
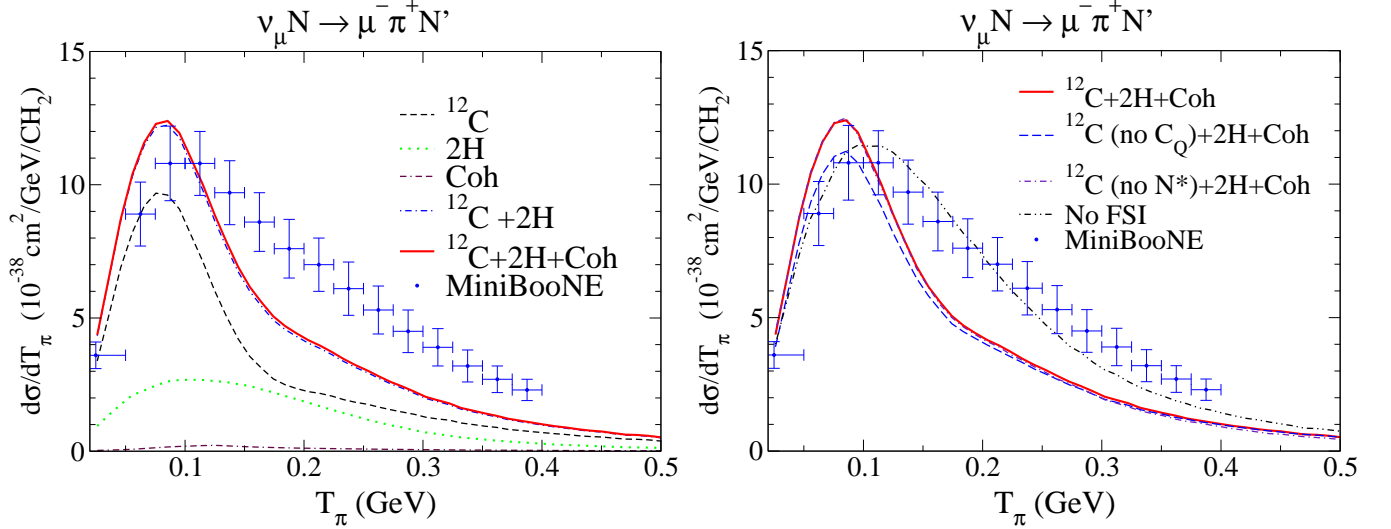

FIG. 7. Flux-folded differential $\frac{d\sigma}{dT_\pi}$ cross section for CC $1\pi^+$ production by ν_μ in mineral oil. Captions as in Fig. 4, but in addition we also display results neglecting FSI (double-dotted dashed line in the right panel) and coherent (short-dashed dotted line in the left panel) contributions. Data from Ref. [3]. Note that the coherent (left panel) and D_{13} resonance (right panel) contributions are very small. The curves obtained when these effects are neglected can hardly be distinguished from the red solid line that stands for the total contribution.

In Fig.8, we show the flux-folded differential $\frac{d\sigma}{dp_\pi}$ and $\frac{d\sigma}{d\cos\theta_\pi}$ cross sections for CC $1\pi^0$ production by ν_μ that we compare to data. For that we use the neutrino flux reported in Ref. [4], that extends from $2\,\mathrm{GeV}$ down to $0.5\,\mathrm{GeV}$ neutrino energies. In this case, there is neither contribution from the hydrogen nuclei nor from coherent production. Once more, the FSI effects are clearly visible in both distributions and their artificial exclusion leads to a better description of the high momentum tail of the $\frac{d\sigma}{dp_\pi}$ distribution. Because of the FSI some pions are absorbed, but other ones are scattered and loose to nucleons part of their energy. FSI is essential to fill the low momentum part of the distribution. From the angular distribution, we see that the pion production off the nucleon model of Ref. [17] leads to a forward peaked cross section. FSI, through quasielastic collisions tends to soften the curve and leads to a better description of the backward scattering. From our point of view, these figures might indicate that some mechanism for pion production, that provides forward high energy pions could be missing in our theoretical scheme.
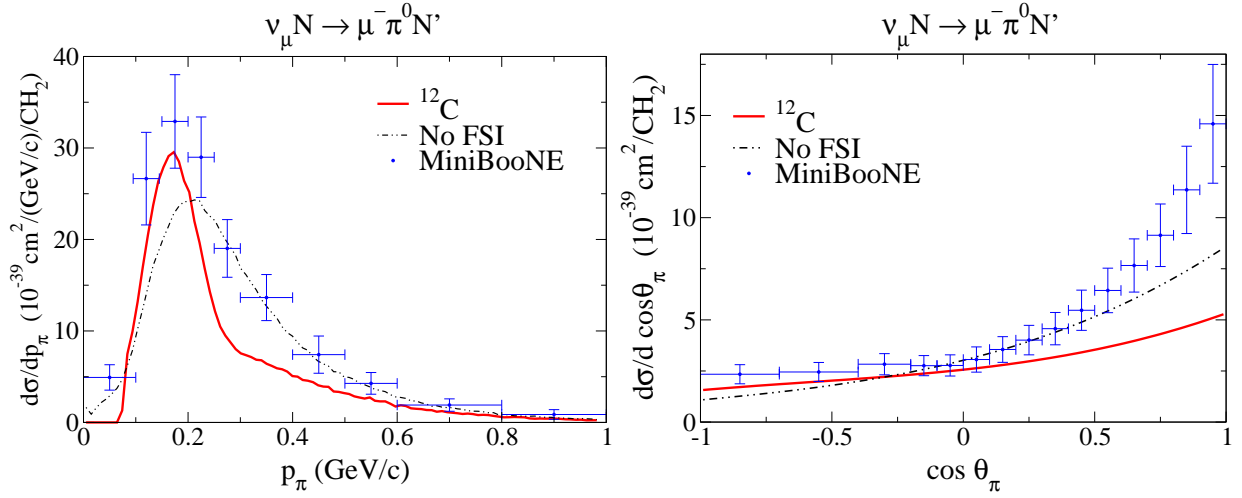
FIG. 8. Flux-folded differential $\frac{d\sigma}{dp_\pi}$ (left panel) and $\frac{d\sigma}{d\cos\theta_\pi}$ (right panel) cross section for $CC\ 1\pi^0$ production by ν_μ in mineral oil. Captions as in Fig. 7. Data from Ref. [4].

B. NC production

In these channels, we compare our model results to data from Ref. [2]. In each case we use the different neutrino/antineutrino fluxes reported by the MiniBooNE collaboration. In Fig. 9, we show the $\frac{d\sigma}{dp_\pi}$ differential cross section and the different contributions coming from ^{12}C, H_2 and the coherent production on ^{12}C. Both for neutrino and antineutrino reactions, we see that the model agrees better with data than in the CC case. We still obtain cross sections below data in the $0.25 \sim 0.5\,\mathrm{GeV/c}$ momentum region. We also see that the role of the D_{13} is negligible while the effects of the C_Q term are small.
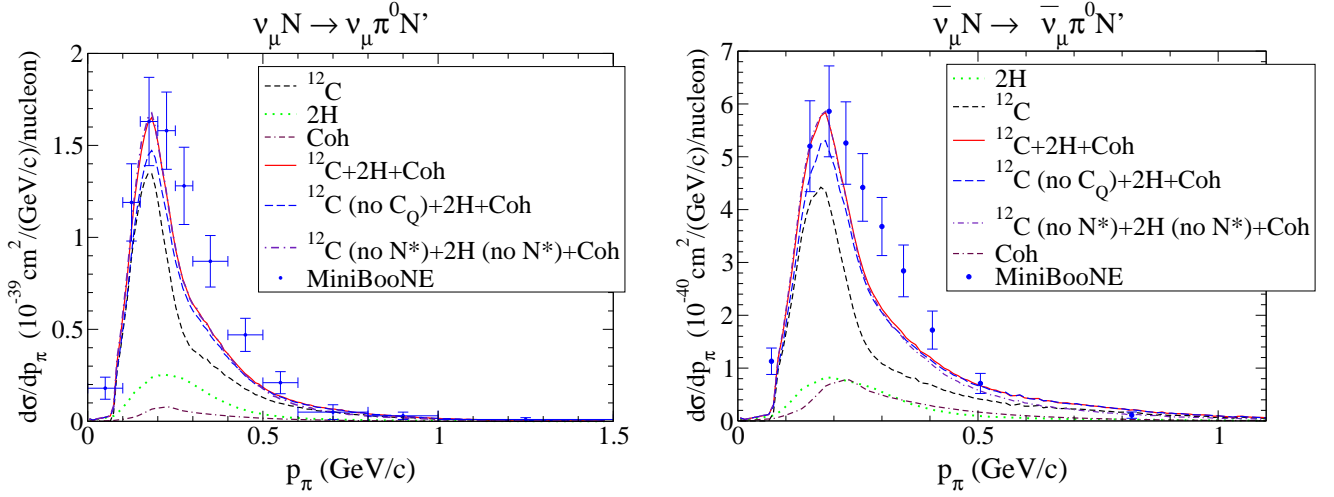

FIG. 9. Flux-folded differential $\frac{d\sigma}{dp_\pi}$ cross section per nucleon for $NC\ 1\pi^0$ production by ν_μ (left panel) and $\bar{\nu}_\mu$ (right panel) in mineral oil. Short-dashed line: ^{12}C contribution. Dotted line: H_2 contribution. Double-dashed dotted line: Coherent contribution. Solid: Full model result. Long-dashed line: ^{12}C contribution without the C_Q term (Eq. (11)). Dashed-dotted line:^{12}C contribution without the D_{13} term. Data from Ref. [2].

In Fig. 10 we show now the flux-folded differential $\frac{d\sigma}{d\cos\theta_\pi}$ cross section. The full model agrees better with data in the antineutrino case where our results are within error bars except in the very forward direction. The role and size of the coherent piece is crucial for the agreement.

There is some deficit for $cos\theta_\pi > 0$ for the reaction with neutrinos but the agreement, as it was the case for the $\frac{d\sigma}{dp_\pi}$ differential cross section, is better than in the corresponding CC reaction. In fact, a minimal enhancement of the
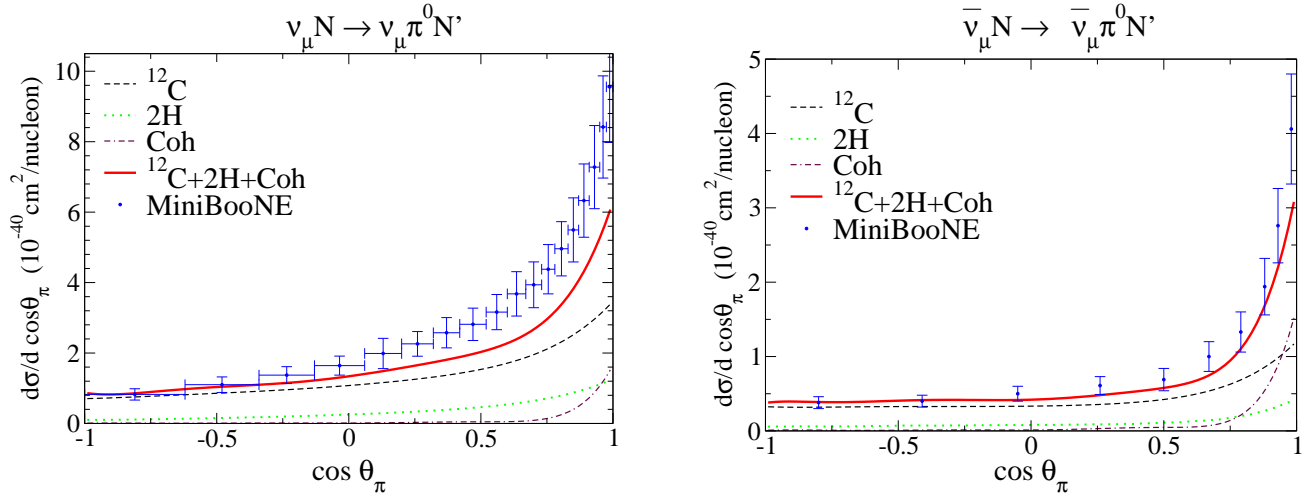
FIG. 10. Flux-folded differential $\frac{d\sigma}{d\cos\theta_\pi}$ cross section per nucleon for $NC\ 1\pi^0$ production by ν_μ (left panel) and $\bar{\nu}_\mu$ (right panel) in mineral oil. Captions as in Fig. 9. Data from Ref. [2].

coherent process and/or the hydrogen contribution, that could be obtained by a larger value of $C_5^A(0)$ also suggested by the CC results, could lead to a better agreement.

IV. CONCLUSIONS

We have extended the model for pion production by neutrinos on nucleons from Refs. [9, 17] by the inclusion of a new term related to the production and decay of the $D_{13}(1520)$ resonance. The resulting model is expected to give a fair reproduction of experimental data on nucleons for neutrino energies up to $2\,\text{GeV}$, always with the uncertainties associated with the poor knowledge of some relevant form factors.

Including nuclear medium corrections that affect both the elementary π production mechanisms and the pion FSI, we have studied pion production by neutrinos in mineral oil in order to compare with recent experimental total and differential cross section measurements. The model provides an overall acceptable description of data, better for NC than for CC channels. In the CC channels, the predicted total cross sections are below data for neutrino energies above $0.8 \sim 0.9\,\text{GeV}$. This result is in agreement with other theoretical calculations [16, 20]. Differential cross sections, folded with the full neutrino flux, show that most of the missing pions lie on the forward direction and at high energies. This might suggest the need of further production mechanisms. NC channels show a better agreement, although theory is also below data. We find that the role of the coherent π production is essential to properly describe the angular distributions in the NC channels. We also find that flux unfolded results seem to support a large value of $C_5^A(0)$, closer to the PCAC prediction than the value obtained from previous combined fits to the ANL and BNL bubble chamber data. Actually, as already discussed in Ref. [20], it seems that MiniBooNE data would be better described using a $C_5^A(0)$ value fitted to BNL data alone.

ACKNOWLEDGMENTS

Appendix A: D_{13} resonance contribution to neutrino-nucleon scattering

In this appendix we give full details of the $D_{13}P$ and $CD_{13}P$ hadronic matrix elements of the $j_{cc+}^\mu(0)$ weak current, depicted in Fig. 3. Those we shall call for short $j_{cc+}^\mu|_{DP}$ and $j_{cc+}^\mu|_{CDP}$.

The matrix element for the direct (DP) contribution is given by

$$j^{\mu}_{cc^+}|_{DP} = iC^{DP}g_D\sqrt{\frac{2}{3}}\cos\theta_C\frac{k^{\alpha}_{\pi}}{p^2_D - M^2_D + iM_D\Gamma_D}\bar{u}(\vec{p}')\gamma_5 P^D_{\alpha\beta}(p_D)\Gamma^{\beta\mu}_D(p,q)\,u(\vec{p}),\ p_D = p+q,\ C^{DP} = \begin{cases} 0 & p\pi^+ \\ 1 & n\pi^+ \end{cases}$$

(A1)

with $M_D = 1520\,\text{MeV}$ the mass of the D_{13} resonance. For g_D we take $g_D = 20\,\text{GeV}^{-1}$ which results from a fit of the $D_{13} \to N\pi$ decay width. For the latter we take 61% of $115\,\text{MeV}$. The width has two main contributions, the $N\pi$ and the $\Delta\pi$ channels. In the propagator we shall use

$$\Gamma_D = \Gamma^{N\pi}_D + \Gamma^{\Delta\pi}_D,$$

where for $\Gamma^{N\pi}_D$ we take

$$\Gamma^{N\pi}_D = \frac{g^2_D}{8\pi}\frac{1}{3s}[(\sqrt{s}-M)^2 - m^2_{\pi}]|\vec{p}_{\pi}|^3\theta(\sqrt{s}-M-m_{\pi}),$$

with $s = p^2_D$ and $|\vec{p}_{\pi}| = \frac{\lambda^{1/2}(s,M^2,m^2_{\pi})}{2\sqrt{s}}$, being $\lambda(a,b,c) = a^2 + b^2 + c^2 - 2ab - 2ac - 2bc$.

For $\Gamma^{\Delta\pi}_D$ we assume an $S-$wave decay and take

$$\Gamma^{\Delta\pi}_D = 0.39 \times 115\,\text{MeV}\frac{|\vec{p}'_{\pi}|}{|\vec{p}'^{o-s}_{\pi}|}\theta(\sqrt{s}-M-m_{\pi}),$$

with $|\vec{p}'_{\pi}| = \frac{\lambda^{1/2}(s,M^2_{\Delta},m^2_{\pi})}{2\sqrt{s}}$ and $|\vec{p}'^{o-s}_{\pi}| = \frac{\lambda^{1/2}(M^2_D,M^2_{\Delta},m^2_{\pi})}{2M_D}$.

Besides,

$$P^D_{\alpha\beta}(p_D) = -(\not{p}_D + M_D)\left[g_{\alpha\beta} - \frac{1}{3}\gamma_{\alpha}\gamma_{\beta} - \frac{2}{3}\frac{p_{D\alpha}p_{D\beta}}{M^2_D} + \frac{1}{3}\frac{p_{D\alpha}\gamma_{\beta} - p_{D\beta}\gamma_{\alpha}}{M_D}\right]$$

(A2)

and

$$\Gamma^{\beta\mu}(p,q) = \left[\frac{\tilde{C}^V_3}{M}\left(g^{\beta\mu}\not{q} - q^{\beta}\gamma^{\mu}\right) + \frac{\tilde{C}^V_4}{M^2}\left(g^{\beta\mu}q\cdot p_D - q^{\beta}p^{\mu}_D\right) + \frac{\tilde{C}^V_5}{M^2}\left(g^{\beta\mu}q\cdot p - q^{\beta}p^{\mu}\right) + \tilde{C}^V_6 g^{\beta\mu}\right]$$
$$+ \left[\frac{\tilde{C}^A_3}{M}\left(g^{\beta\mu}\not{q} - q^{\beta}\gamma^{\mu}\right) + \frac{\tilde{C}^A_4}{M^2}\left(g^{\beta\mu}q\cdot p_D - q^{\beta}p^{\mu}_D\right) + \tilde{C}^A_5 g^{\beta\mu} + \frac{\tilde{C}^A_6}{M^2}q^{\beta}q^{\mu}\right]\gamma_5,\ \ p_D = p+q.$$

(A3)

The axial form factors are taken from Ref. [26]

$$\tilde{C}^A_3 = \tilde{C}^A_4 = 0,\ \ \tilde{C}^A_5 = \frac{-2.1}{(1-q^2/M^2_A)^2}\frac{1}{1-q^2/(3M^2_A)},\ \ \tilde{C}^A_6(q^2) = \tilde{C}^A_5(q^2)\frac{M^2}{m^2_{\pi} - q^2},\ \ M_A = 1\,\text{GeV},$$

(A4)

while for the vector ones we fitted the form factor results in Ref. [52] to get

$$\tilde{C}^V_3 = \frac{-2.98}{[1-q^2/(1.4M^2_V)]^2},\ \ \tilde{C}^V_4 = \frac{4.21/D_V}{1-q^2/(3.7M^2_V)},\ \ \tilde{C}^V_5 = \frac{-3.13/D_V}{1-q^2/(0.42M^2_V)},\ \ \tilde{C}^V_6 = 0,$$

(A5)

with $M_V = 0.84\,\text{GeV}$ and $D_V = (1-q^2/M^2_V)^2$.

For the crossed CDP contribution we have

$$j^{\mu}_{cc^+}|_{CDP} = -iC^{CDP}g_D\sqrt{\frac{2}{3}}\cos\theta_C\frac{k^{\alpha}_{\pi}}{p^2_D - M^2_D + iM_D\Gamma_D}\bar{u}(\vec{p}')\hat{\Gamma}^{\mu\beta}_D(p',-q)\,P^D_{\beta\alpha}(p_D)\gamma_5 u(\vec{p})$$

(A6)

with

$$p_D = p' - q\ ,\ \ C^{CDP} = \begin{cases} 1 & p\pi^+ \\ 0 & n\pi^+ \end{cases}$$

(A7)

and

$$\hat{\Gamma}^{\mu\beta}_D(p',-q) = \gamma^0[\Gamma^{\beta\mu}_D(p',-q)]^{\dagger}\gamma^0.$$

From isospin symmetry we further have [17]

$$\langle p\pi^0|j_{cc+}^\mu(0)|n\rangle = -\frac{1}{\sqrt{2}}\Big[\langle p\pi^+|j_{cc+}^\mu(0)|p\rangle - \langle n\pi^+|j_{cc+}^\mu|n\rangle\Big],$$

$$\langle p\pi^-|j_{cc-}^\mu(0)|p\rangle = \langle n\pi^+|j_{cc+}^\mu|n\rangle,$$

$$\langle n\pi^-|j_{cc-}^\mu(0)|n\rangle = \langle p\pi^+|j_{cc+}^\mu|p\rangle.$$

For NC neutrino and antineutrino induced reactions the contribution from the D_{13} has isovector plus isoscalar parts. The isovector (IV) part is related to the CC processes and is given by (see discussion on Sec. III of Ref. [17])

$$\langle p\pi^0|j_{nc,\mathrm{IV}}^\mu(0)|p\rangle = \frac{1}{\sqrt{2}\cos\theta_C}\Big\{ (1-2\sin^2\theta_W)\Big[\langle p\pi^+|V_{cc+}^\mu(0)|p\rangle + \langle n\pi^+|V_{cc+}^\mu(0)|n\rangle\Big]$$
$$-\Big[\langle p\pi^+|A_{cc+}^\mu(0)|p\rangle + \langle n\pi^+|A_{cc+}^\mu(0)|n\rangle\Big]\Big\},$$

$$\langle n\pi^+|j_{nc,\mathrm{IV}}^\mu(0)|p\rangle = -\frac{1}{\cos\theta_C}\Big\{ (1-2\sin^2\theta_W)\Big[\langle p\pi^+|V_{cc+}^\mu(0)|p\rangle - \langle n\pi^+|V_{cc+}^\mu(0)|n\rangle\Big]$$
$$-\Big[\langle p\pi^+|A_{cc+}^\mu(0)|p\rangle - \langle n\pi^+|A_{cc+}^\mu(0)|n\rangle\Big]\Big\},$$

$$\langle n\pi^0|j_{nc,\mathrm{IV}}^\mu(0)|n\rangle = \langle p\pi^0|j_{nc,\mathrm{IV}}^\mu(0)|p\rangle,$$

$$\langle p\pi^-|j_{nc,\mathrm{IV}}^\mu(0)|n\rangle = -\langle n\pi^+|j_{nc,\mathrm{IV}}^\mu(0)|p\rangle.$$

where we have written $j_{cc+}^\mu(0) = V_{cc+}^\mu(0) - A_{cc+}^\mu(0)$ being $V_{cc+}^\mu(0)$ and $A_{cc+}^\mu(0)$ respectively the vector and axial part of the current.

The isoscalar current is given in terms of the isoscalar part of the electromagnetic current as

$$j_{nc,\mathrm{IS}}^\mu(0) = -4\sin^2\theta_W\, s_{em,\mathrm{IS}}^\mu(0),$$

and one has (see discussion on Sec. III of Ref. [17])

$$\langle n\pi^+|s_{em,\mathrm{IS}}^\mu(0)|p\rangle = \langle p\pi^-|s_{em,\mathrm{IS}}^\mu(0)|n\rangle = \sqrt{2}\,\langle p\pi^0|s_{em,\mathrm{IS}}^\mu(0)|p\rangle = -\sqrt{2}\,\langle n\pi^0|s_{em,\mathrm{IS}}^\mu(0)|n\rangle.$$

The direct contribution to $\frac{1}{2}[\langle n\pi^0|s_{em,\mathrm{IS}}^\mu(0)|n\rangle - \langle p\pi^0|s_{em,\mathrm{IS}}^\mu(0)|p\rangle]$ is given by

$$-ig_D\frac{1}{\sqrt{3}}\frac{1}{p_D^2-M_D^2+iM_D\Gamma_D}\frac{k_\pi^\alpha}{}\,\bar{u}(\vec{p}')\gamma_5 P_{\alpha\beta}^D(p_D)\Gamma_D^{V,\mathrm{IS}\,\beta\mu}(p,q)\,u(\vec{p}),\ \ p_D = p+q,$$

and

$$\Gamma_D^{V,\mathrm{IS}\,\beta\mu} = \left[\frac{\tilde{C}_3^{V,\mathrm{IS}}}{M}\left(g^{\beta\mu}\slashed{q}-q^\beta\gamma^\mu\right) + \frac{\tilde{C}_4^{V,\mathrm{IS}}}{M^2}\left(g^{\beta\mu}q\cdot p_D - q^\beta p_D^\mu\right) + \frac{\tilde{C}_5^{V,\mathrm{IS}}}{M^2}\left(g^{\beta\mu}q\cdot p - q^\beta p^\mu\right) + \tilde{C}_6^{V,\mathrm{IS}}g^{\beta\mu}\right]$$

with

$$\tilde{C}_3^{V,\mathrm{IS}} = \frac{-1.21}{[1-q^2/(1.4M_V^2)]^2},\quad \tilde{C}_4^{V,\mathrm{IS}} = \frac{0.515/D_V}{1-q^2/(3.7M_V^2)},\quad \tilde{C}_5^{V,\mathrm{IS}} = \frac{0.395/D_V}{1-q^2/(0.42M_V^2)},\quad \tilde{C}_6^{V,\mathrm{IS}} = 0,$$

with their values at $q^2=0$ extracted from Ref. [52].

The crossed contribution to $\frac{1}{2}[\langle n\pi^0|s_{em,\mathrm{IS}}^\mu(0)|n\rangle - \langle p\pi^0|s_{em,\mathrm{IS}}^\mu(0)|p\rangle]$ is given by

$$ig_D\frac{1}{\sqrt{3}}\frac{1}{p_D^2-M_D^2+iM_D\Gamma_D}\frac{k_\pi^\alpha}{}\,\bar{u}(\vec{p}')\hat{\Gamma}_D^{V,\mathrm{IS}\,\mu\beta}(p',-q) P_{\beta\alpha}^D(p_D)\gamma_5 u(\vec{p}),\ \ p_D = p'-q,$$

with

$$\hat{\Gamma}_D^{V,\mathrm{IS}\,\mu\beta}(p',-q) = \gamma^0[\Gamma_D^{V,\mathrm{IS}\,\beta\mu}(p',-q)]^\dagger\gamma^0.$$

[1] E. Fernandez-Martinez, D. Meloni and , Phys. Lett. B **697**, 477 (2011).
[2] A. A. Aguilar-Arevalo *et al.* [MiniBooNE Collaboration], Phys. Rev. D **81**, 013005 (2010).

[3] A. A. Aguilar-Arevalo *et al.* [MiniBooNE Collaboration], Phys. Rev. D **83**, 052007 (2011).

[4] A. A. Aguilar-Arevalo *et al.* [MiniBooNE Collaboration], Phys. Rev. D **83**, 052009 (2011).

[5] J. Campbell, G. Charlton, Y. Cho, M. Derrick, R. Engelmann, J. Fetkovich, L. Hyman and K. Jaeger *et al.*, Phys. Rev. Lett. **30**, 335 (1973).

[6] G. M. Radecky, V. E. Barnes, D. D. Carmony, A. F. Garfinkel, M. Derrick, E. Fernandez, L. Hyman and G. Levman *et al.*, Phys. Rev. D **25**, 1161 (1982) [Erratum-ibid. D **26**, 3297 (1982)].

[7] T. Kitagaki, H. Yuta, S. Tanaka, A. Yamaguchi, K. Abe, K. Hasegawa, K. Tamai and S. Kunori *et al.*, Phys. Rev. D **34**, 2554 (1986).

[8] L. Alvarez-Ruso, S. K. Singh and M. J. Vicente Vacas, Phys. Rev. C **59**, 3386 (1999) [nucl-th/9804007].

[9] E. Hernandez, J. Nieves, M. Valverde and M. J. Vicente Vacas, Phys. Rev. D **81**, 085046 (2010).

[10] J. G. Morfin, J. Nieves, J. T. Sobczyk and , Adv. High Energy Phys. **2012**, 934597 (2012).

[11] T. Golan, C. Juszczak and J. T. Sobczyk, Phys. Rev. C **86**, 015505 (2012).

[12] D. Rein and L. M. Sehgal, Nucl. Phys. B **223**, 29 (1983).

[13] J. E. Amaro, E. Hernandez, J. Nieves and M. Valverde, Phys. Rev. D **79**, 013002 (2009).

[14] C. Berger, L. M. Sehgal and , Phys. Rev. D **79**, 053003 (2009).

[15] E. Hernandez, J. Nieves, M. J. Vicente-Vacas and , Phys. Rev. D **80**, 013003 (2009).

[16] J. T. Sobczyk. and J. Zmuda, arXiv:1210.6149 [nucl-th].

[17] E. Hernandez, J. Nieves and M. Valverde, Phys. Rev. D **76**, 033005 (2007).

[18] T. Leitner, O. Buss, L. Alvarez-Ruso and U. Mosel, Phys. Rev. C **79**, 034601 (2009).

[19] MAID, http://wwwkph.kph.uni-mainz.de/

[20] O. Lalakulich and U. Mosel, Phys. Rev. C **87**, 014602 (2013).

[21] T. Leitner, O. Lalakulich, O. Buss, U. Mosel and L. Alvarez-Ruso, AIP Conf. Proc. **1222** (2010) 212 [arXiv:0910.2835 [nucl-th]].

[22] T. Leitner, O. Buss, U. Mosel and L. Alvarez-Ruso, AIP Conf. Proc. **1189** (2009) 207 [arXiv:0909.0838 [nucl-th]].

[23] L. L. Salcedo, E. Oset, M. J. Vicente-Vacas and C. Garcia-Recio, Nucl. Phys. A **484**, 557 (1988).

[24] C. H. Llewellyn Smith, Phys. Rept. **3**, 261 (1972).

[25] P. A. Schreiner and F. Von Hippel, Phys. Rev. Lett. **30**, 339 (1973).

[26] O. Lalakulich, E. A. Paschos and G. Piranishvili, Phys. Rev. D **74**, 014009 (2006).

[27] S. L. Adler, Annals Phys. **50**, 189 (1968).

[28] E. A. Paschos, J. -Y. Yu and M. Sakuda, Phys. Rev. D **69**, 014013 (2004). [hep-ph/0308130].

[29] K. M. Graczyk, D. Kielczewska, P. Przewlocki and J. T. Sobczyk, Phys. Rev. D **80**, 093001 (2009).

[30] R. C. Carrasco, E. Oset and , Nucl. Phys. A **536**, 445 (1992).

[31] R. C. Carrasco, E. Oset and L. L. Salcedo, Nucl. Phys. A **541**, 585 (1992).

[32] A. Gil, J. Nieves and E. Oset, Nucl. Phys. A **627**, 543 (1997).

[33] A. Gil, J. Nieves and E. Oset, Nucl. Phys. A **627**, 599 (1997).

[34] J. Nieves, I. Ruiz Simo and M. J. Vicente Vacas, Phys. Rev. C **83**, 045501 (2011).

[35] M. Hirata, J. H. Koch, E. J. Moniz and F. Lenz, Annals Phys. **120**, 205 (1979).

[36] E. Oset and L. L. Salcedo, Nucl. Phys. A **468**, 631 (1987).

[37] J. Nieves, E. Oset and C. Garcia-Recio, Nucl. Phys. A **554**, 509 (1993).

[38] O. Benhar, N. Farina, H. Nakamura, M. Sakuda and R. Seki, Phys. Rev. D **72**, 053005 (2005).

[39] L. Alvarez-Ruso, L. S. Geng, S. Hirenzaki and M. J. Vicente Vacas, Phys. Rev. C **75**, 055501 (2007) [Erratum-ibid. C **80**, 019906 (2009)].

[40] A. A. Aguilar-Arevalo *et al.* [MiniBooNE Collaboration], Phys. Rev. D **81**, 092005 (2010).

[41] E. Hernandez, J. Nieves and M. Valverde, Phys. Rev. D **82**, 077303 (2010).

[42] J. Nieves, E. Oset and C. Garcia-Recio, Nucl. Phys. A **554**, 554 (1993).

[43] E. Oset, P. Fernandez de Cordoba, L. L. Salcedo and R. Brockmann, Phys. Rept. **188**, 79 (1990).

[44] M. J. Vicente Vacas and E. Oset, Nucl. Phys. A **568**, 855 (1994).

[45] R. C. Carrasco, M. J. Vicente Vacas and E. Oset, Nucl. Phys. A **570**, 701 (1994).

[46] H. C. Chiang, E. Oset and P. Fernandez de Cordoba, Nucl. Phys. A **510**, 591 (1990).

[47] Y. Ashie *et al.* [Super-Kamiokande Collaboration], Phys. Rev. D **71**, 112005 (2005).

[48] M. H. Ahn *et al.* [K2K Collaboration], Phys. Rev. D **74**, 072003 (2006).

[49] K. Abe *et al.* [T2K Collaboration], Phys. Rev. Lett. **107**, 041801 (2011).

[50] S. K. Singh, M. Sajjad Athar, S. Ahmad and , Phys. Rev. Lett. **96**, 241801 (2006).

[51] L. Alvarez-Ruso, L. S. Geng, M. J. Vicente Vacas and , Phys. Rev. C **76**, 068501 (2007) [Erratum-ibid. C **80**, 029904 (2009)].

[52] T. J. Leitner, "Neutrino-nucleus interactions in a coupled-channel hadronic transport model". University of Giessen Thesis, 2009. A copy can be retrieved from the webpage http://gibuu.physik.uni-giessen.de/GiBUU/wiki/Paper#PhDtheses.